Computers & Geosciences 100 (2017) 1–9

Contents lists available at ScienceDirect

Computers & Geosciences

journal homepage: www.elsevier.com/locate/cageo

A tetrahedral mesh generation approach for 3D marine controlled-source electromagnetic modeling

Evan Schankee Um[a], Seung-Sep Kim[b], Haohuan Fu[c,d,*]

[a] Affiliate of Earth and Environmental Sciences, Lawrence Berkeley National Laboratory, CA, USA
[b] Geology and Earth Environmental Sciences, Chungnam National University, Daejeon, South Korea
[c] Tsinghua University, Ministry of Education Key Laboratory for Earth System Modeling and Center for Earth System Science, Beijing, China
[d] National Supercomputing Center in Wuxi, Wuxi, China

ARTICLE INFO

Keywords:
Marine electromagnetic geophysics
Finite element modeling
Parallel computing

ABSTRACT

3D finite-element (FE) mesh generation is a major hurdle for marine controlled-source electromagnetic (CSEM) modeling. In this paper, we present a FE discretization operator (FEDO) that automatically converts a 3D finite-difference (FD) model into reliable and efficient tetrahedral FE meshes for CSEM modeling. FEDO sets up wireframes of a background seabed model that precisely honors the seafloor topography. The wireframes are then partitioned into multiple regions. Outer regions of the wireframes are discretized with coarse tetrahedral elements whose maximum size is as large as a skin depth of the regions. We demonstrate that such coarse meshes can produce accurate FE solutions because numerical dispersion errors of tetrahedral meshes do not accumulate but oscillates. In contrast, central regions of the wireframes are discretized with fine tetrahedral elements to describe complex geology in detail. The conductivity distribution is mapped from FD to FE meshes in a volume-averaged sense. To avoid excessive mesh refinement around receivers, we introduce an effective receiver size. Major advantages of FEDO are summarized as follow. First, FEDO automatically generates reliable and economic tetrahedral FE meshes without adaptive meshing or interactive CAD workflows. Second, FEDO produces FE meshes that precisely honor the boundaries of the seafloor topography. Third, FEDO derives multiple sets of FE meshes from a given FD model. Each FE mesh is optimized for a different set of sources and receivers and is fed to a subgroup of processors on a parallel computer. This divide and conquer approach improves the parallel scalability of the FE solution. Both accuracy and effectiveness of FEDO are demonstrated with various CSEM examples.

1. Introduction

In the past decade, 3D finite-element (FE) solutions have been widely used in marine controlled-source electromagnetic (CSEM) modeling (e.g. Key and Ovall, 2011; Schwarzbach et al., 2011). In contrast to finite-difference (FD) solutions that approximate non-coordinate-conforming structures with small rectangular stair steps, FE uses geometry-conforming tetrahedral meshes and precisely represents complex seafloor topography.

However, the advantage of FE over FD comes with extra complication. It is considered difficult to iteratively solve a system of FE equations. A system matrix with tetrahedra is unstructured and not diagonally dominant. A simple Jacobi preconditioner used in FD solutions does not ensure convergence of FE Krylov solutions. FE solutions require numerically expensive preconditioners such as incomplete factorization (Um et al., 2013) and others. It is also difficult to find a robust preconditioner suitable to a wide range of EM problems. Accordingly, direct solvers are often the method of choice for FE solutions despite their large memory requirements and low parallel scalabilities (Fu et al., 2015).

It is also considered difficult and time-consuming to create 3D FE meshes. 3D FE mesh generation requires good literacy in computer-aided design (CAD) software that may have a steep learning curve. To mitigate the difficulty, adaptive FE methods have been introduced (Li and Key, 2007; Key and Ovall, 2011; Schwarzbach et al., 2011). They start with coarse meshes and successively refine meshes until a required tolerance is met. However, in either use of interactive CAD or automated adaptive refinement methods, it is nontrivial to generate reliable and efficient 3D meshes for a complex multi-scale model.

The goal of this paper is to present a 3D FE discretization operator (FEDO) that automatically generates reliable and efficient tetrahedral meshes for marine CSEM. We develop strategies for directly creating

* Corresponding author.
E-mail addresses: evanum@gmail.com (E.S. Um), seungsep@cnu.ac.kr (S.-S. Kim), haohuan@tsinghua.edu.cn (H. Fu).

http://dx.doi.org/10.1016/j.cageo.2016.11.007
Received 4 August 2016; Received in revised form 17 November 2016; Accepted 20 November 2016
Available online 21 November 2016
0098-3004/ © 2016 Elsevier Ltd. All rights reserved.

complete FE meshes without adaptive refinement. The development requires understanding basic properties of tetrahedral meshes for diffusive EM modeling, which are often not obvious when CAD or adaptive refinement methods are employed. Ultimately, we aim to demonstrate that FEDO can quickly derive accurate and efficient FE meshes from a given seabed model without computational overhead associated with adaptive mesh refinement or interactive CAD works.

The remainder of this paper is organized as follows. We first review the FE formulation for CSEM. Its numerical dispersion characteristics are examined to determine proper tetrahedral sizes. To avoid excessive mesh refinement around receivers, we introduce an effective receiver size. We follow this by presenting a matrix that maps conductivity from FD model to FE simulation meshes. The three components above are casted into FEDO. Finally, we apply FEDO to complex offshore models, compute their CSEM solutions and demonstrate its accuracy and efficiency.

2. Finite element formulation

Since the discretization density required for accurate EM solutions is directly related with an FE formulation, we briefly describe the total field FE formulation (Um et al., 2013) used here. The electric-field diffusion equation is given by

$$\frac{1}{\mu_o}\nabla\times\nabla\times\mathbf{e}(\mathbf{r})+\hat{j}\,\omega\sigma\mathbf{e}(\mathbf{r})+\hat{j}\,\omega\mathbf{J}_s(\mathbf{r})=0, \tag{1}$$

where $\mathbf{e}(\mathbf{r})$ is the electric field at position $\mathbf{r}$, $\mathbf{J}_s(\mathbf{r})$ is an electric source at an angular frequency ω, μ_o is the magnetic permeability of free space ($4\pi\times10^{-7}$ H/m), and σ is the conductivity. The development of the equivalent weak statement of Eq. (1) requires the multiplication of Eq. (1) by the edge basis function and the integration over the model domain of $\mathbf{V}$, resulting in

$$\iiint_{V^e}\mathbf{n}_i^e(\mathbf{r})\cdot\left(\frac{1}{\mu_o}\nabla\times\nabla\times\mathbf{e}^e(\mathbf{r})+\hat{j}\,\omega\sigma^e\mathbf{e}^e(\mathbf{r})+\hat{j}\,\omega\mathbf{J}_s(\mathbf{r})\right)dV=0. \tag{2}$$

The superscript e denotes the e$^{\text{th}}$ tetrahedral element, $\mathbf{n}_i^e(\mathbf{r})$ with i varying from 1 to 6 is a set of edge basis functions. V^e is the volume of the eth element. $\mathbf{n}_i^e(\mathbf{r})$ is also chosen as the basis. Thus, the electric field at a point inside or on a given element is expanded as

$$\mathbf{e}^k(\mathbf{r})=\sum_{j=1}^{6}\mathbf{e}_j^k(\mathbf{r})=\sum_{j=1}^{6}u_j^k\mathbf{n}_j^k(\mathbf{r}), \tag{3}$$

where u_j^k is the unknown amplitude of the electric field on the jth edge of the kth element. Accordingly, the FE method is the second-order accurate (Jin and Riley, 2008).

Substituting Eq. (3) into Eq. (2) and using the homogeneous Dirichlet boundary conditions yield

$$(\mathbf{A}^e+\mu_o\omega\hat{j}\,\mathbf{B}^e)\mathbf{u}^e=-\mu_o\omega\hat{i}\,\mathbf{s}^e \tag{4}$$

where

$$(i,j)\text{ element of }\mathbf{A}^e=\iiint_{V^e}\nabla\times\mathbf{n}_i^e(\mathbf{r})\cdot\nabla\times\mathbf{n}_j^e(\mathbf{r})dV, \tag{5}$$

$$(i,j)\text{ element of }\mathbf{B}^e=\iiint_{V^e}\mathbf{n}_i^e(\mathbf{r})\cdot\sigma^e\mathbf{n}_j^e(\mathbf{r})dV, \tag{6}$$

$$i\text{ element of }\mathbf{s}^e=\iiint_{V^e}\mathbf{n}_i^e(\mathbf{r})\cdot\mathbf{J}_s(\mathbf{r})dV, \tag{7}$$

$$\mathbf{u}^e=[u_1^e\ \ u_2^e\ \ \dots\ \ u_6^e]. \tag{8}$$

Eq. (4) is considered local as it results from integration over each element. The local systems from all elements are assembled into a single global system of equations. The global system is solved using a parallel direct solver.

Table 1
δ and λ in the seawater.

f (Hz)	δ (m)	λ (m)
0.10	873.0	5484.9
0.15	712.8	4478.4
0.20	617.3	3878.4
0.25	552.1	3469.0
0.30	504.0	3166.7
0.35	466.6	2931.8
0.40	436.5	2742.5
0.45	411.5	2585.6
0.50	390.4	2452.9

3. Numerical dispersion analysis

To determine tetrahedral mesh density required for accurate solutions, we examine numerical dispersion characteristics for a homogeneous whole-space seawater (3.33 S/m) model. We are interested in efficient discretization of the seawater because the seawater can be a large portion of a CSEM model and requires the smallest elements due to its highest conductivity. The seawater model is 20×10×10 km in the x-, y- and z-direction, respectively. The lower left corner of the model is at (−5, −5, 5 km). A 250 m long x-oriented electric source is placed at (0, 0, 0 km). 20 m long x-oriented electric receivers are placed with 1 km spacing from x=1−10 km. We consider nine source frequencies from 0.1 to 0.5 Hz with 0.05 Hz interval. Skin depth (δ) and wavelength (λ) of the seawater are presented in Table 1.

The model (Fig. 1) is discretized using tetrahedral elements whose vary from 10 m (near sources and receivers) to 400 m (most areas). This is slightly smaller than δ at 0.3 Hz. Note that the FE meshes are refined around not only the source but also the receivers. This is one of the major differences between FD and FE. The mesh refinement near the receivers will be discussed in the next section. The transition from small to large edges is controlled by the growth factor defined as the maximum rate at which the edge size can grow. The growth factor is typically 1.5–2.0 from one edge to the next.

Amplitudes, relative amplitude errors and phases of FE solutions are plotted against analytic solutions in Fig. 2a-c, respectively. The relative errors are defined by ‖(numerical solution−analytic solution)/analytic solution)‖. It is assumed that over 10 km source-receiver offset, 5% amplitude errors are accurate enough. Based on the criterion, the FE meshes support the lowest four frequencies: 0.10, 0.15, 0.20 and 0.25 Hz. At 0.10 Hz, the boundary effects appear at x=8 km. To highlight the numerical dispersion characteristics of the FE meshes, we also repeat the same experiments with a 2nd-order accurate FD method (Newman and Alumbaugh, 1995). The FD grid size is set to 400 m as same as that in the FE meshes. However, FD does not produce accurate solutions at all nine frequencies (not included here). We reduce the FD grid to 100 m and analyze amplitudes, their relative errors and phases (Fig. 2d–f). Due to their geometric simplicity, the FD grids are not presented here. The FD grids support the lowest four frequencies (Fig. 2e). At 0.10 Hz, the boundary

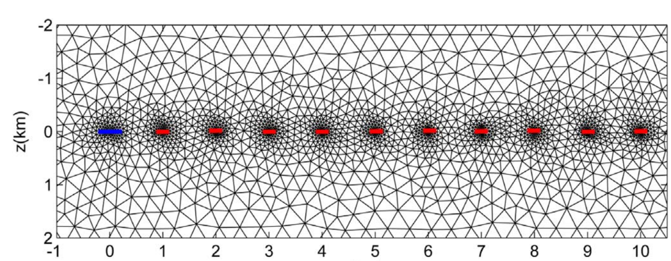

Fig. 1. The FE meshes for the seawater model. Blue and red lines represent source and receivers, respectively. (For interpretation of the references to color in this figure legend, the reader is referred to the web version of this article.)

Download English Version:

https://daneshyari.com/en/article/4965389

Download Persian Version:

https://daneshyari.com/article/4965389

Daneshyari.com